

Detection and Removal of Line Scratches in Motion Picture Films

L. Joyeux, O. Buisson, B. Besserer, S. Boukir

ljoyeux@gi.univ-lr.fr, obuisson@gi.univ-lr.fr, bbessere@gi.univ-lr.fr, sboukir@gi.univ-lr.fr

Laboratoire d'Informatique et d'Imagerie Industrielle (L3i)
Université de La Rochelle, avenue Marillac, F-17042 La Rochelle cedex 1, France

Abstract

Line scratches are common degradations in motion picture films. This paper presents an efficient method for line scratches detection strengthened by a Kalman filter. A new interpolation technique, dealing with both low and high frequencies (i.e. film grain) around the line artifacts, is investigated to achieve a nearby invisible reconstruction of damaged areas. Our line scratches detection and removal techniques have been validated on several film sequences.

1 Introduction

Motion picture industry is 100 years old and chemical film (nowadays polyester, former triacetate or nitrate) is still the main support for motion picture film, despite of fast-growing digital media. It is a fact the film and dye coating for color are not stable over decades. In addition, some old films are reassembled from fragments scattered over various libraries and archives. Only digital processing will ensure the removal of the various artifacts due to age and a well balanced output to a film recorder. The major artifacts damaging B&W films are :

- **Dust spots and thin hair:** primarily caused by careless handling, poorly maintained equipment and improper storage. Dust spots are randomly spread over each frame, and disturb the viewer when too numerous.
- **Scratches and abrasions:** non photographic blemishes on the film emulsion or base, due to film slippage during fast start, stops and rewinding, therefore scratching the film with accumulated dirt particles. Because the scratch is spread over many frames, and appears at same location during projection, this kind of film damage is readily seen by the viewer.
- **Spatial instabilities:** caused by damage at the corners of the perforations, misalignment of film in the projector (scanner) gate, improper film guidance in old cameras.

- **Intensity instabilities:** due to jerky shutter control and film transport by old hand crank cameras. In recent movies, the cause is often non synchronized light sources. Sometimes, a gray shadow due to mishandling during the chemical development process induces similar intensity variation.

Of course, this list is non exhaustive (large roping, color dye attenuation, etc.).

A large number of films are digitized for TV broadcasting, using *telecine*. Usually, the print goes through a wet gate and the low output resolution (720×576 in Europe) allows low pass or median filtering [14], [10]. Dust spots and scratches will nearby disappear, and large artifacts are removed with specialized (and real-time for video resolution) hardware.

Digital processing will be different if the frames are shoot back again on 35mm film after processing. Such a process is also common for digital special effects (FXs). Digital FXs are expensive, need high computational power and have to be controlled by an operator. On most cases, only a short footage of the whole movie relies on digital. For motion picture film restoration, we need full quality digital processing on 2K or 4K images over the whole footage. Therefore, processing power have to be cheap, processing time as short as possible and the restoration process should be **automated**, to cut exploitation costs.

Our digital restoration is a three-stage process. The first stage is a detection process, running without human interaction on the raw image sequence. Motion compensation is computed during this step, and relevant information stored. An efficient algorithm for motion compensation [2], fast enough on 2K images, is the core of many of our detection algorithms (spatial instabilities, intensity instabilities and dust detection). During the second step, an operator checks the results of the detection process. The last step is automatic again. According to parameters set up by the operator, the image sequence is processed again. Using image masks and data generated during the detection step, artifacts are removed.

Nowadays, our challenge is automatic line scratches detection and removal. Unlike dust particles which are randomly spread over a frame, line scratches remain at nearby

the same location over frames. Therefore, these artifacts are not "seen" by the motion compensation algorithm.

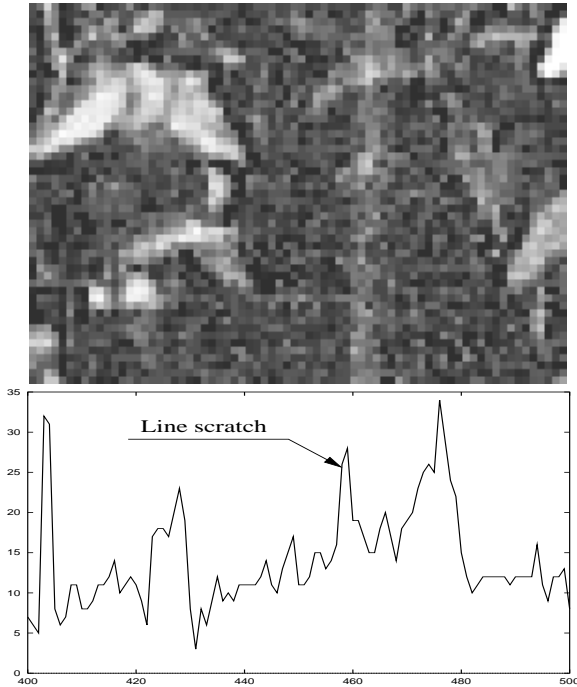


Figure 1: Enlarged part of a frame. Noise (film grain, scanner artifacts or video noise if *telecine*) is visible. Below, corresponding line scratch profile

2 Line scratch features

Line scratches are easily visible as vertical lines of bright or dark intensity, oriented more or less vertically over much of the image.

Following line scratch features should be extracted from the digital image : location with respect to the x-axis, angle to the vertical, width. The length or duration of a line scratch is unknown (less than a frame up to a whole reel) and sometimes periodical, hence detecting the beginning and the trailing of a scratch is a special case.

Unlike Kokaram who uses only one frame to detect line scratches [6], we focus on temporal features, even for not perfectly vertical line scratches (see fig. 1). Indeed, one has to check the behavior of potential line artifacts over the film sequence to reject false detections.

3 Line scratch detection

3.1 Projection before detection

A scratch is a local minimum of the intensity curve along the x-axis. Film grain, dust spots and scanner artifacts introduce noise as shown on fig. 1. We use Radon

projections along the y-axis to minimize noise influence [11].



Figure 2: *Telecine* example (720x576) showing a small scratch (in fact, only visible in the blue plane) and corresponding raw, untracked, detection using 16 pixel-height projected stripes

Given a grey scale image, I , our data projections may be expressed as :

$$\mathcal{P}_H(x, i) = \sum_{j=0}^{H-1} I(x, j + H \cdot i) \quad (1)$$

Projection height H is estimated in relation with the greatest acceptable angle to the vertical and the image resolution. All subsequent work up to the artifacts detection uses these projected stripes.

3.2 Spatial line scratch detection

In previous work, we have proposed a simple method for detecting local minima [2]. This approach relies on grey scale morphological transformations (closing and opening) [12]. Our local minima detector is expressed as a simple

difference between the original image and its closing :

$$D(I(x, y), M) = ((I(x, y) \oplus M) \ominus M) - I(x, y) \quad (2)$$

where M denotes the structuring element.

As this technique worked well for local deteriorations detection such as blotches [2], we try to apply it to the case of line artifacts.

Local minima within each projected strip are then detected using the previous morphological detector. The structuring element should be large enough, according to image resolution, to completely detect the scratches. These structuring elements are not flat, but constrained : $M(x) = N|x|, x \in [-a, a]$. If a is low, this detector reacts to noise, otherwise the localization is imprecise. If the value of N is too large, sharp edges will be assimilated to line scratches. Therefore, finding correct values for a and N for the complete sequence is not easy, and does not contribute to full automatic processing. However, this basic method may be strengthened by a tracking process. Therefore, the parameters are fixed to low values in order to detect every line scratch. Of course, this will increase the number of wrong detections. But, the tracking process will eliminate them. Let us emphasize that even if the static detection worked perfectly, temporal behavior of the potential artifacts has to be checked to reject lines occurring as a natural part of the images.

Figure 2 shows the result of our spatial line scratch detection algorithm. Only the positions of the middle of the detected potential line scratches are depicted, their width are not represented for better illustration. A great number of false detections is obtained due on the one hand to the use of low thresholds and, on the other hand, to the high intensity of noise which makes the detection process very complicated on this film sequence (this noise is much more apparent in a zoomed part of this original frame depicted on fig. 1).

4 Line scratch tracking

In this section, we aim at tracking the detected artifact lines over the image sequence to refine the previous spatial detection process. An accurate detection field may be achieved to allow a suitable reconstruction of the deteriorated areas. Indeed, the first detection step only provides an approximate detection field which may contain false detections. A powerful technique for doing such tracking process is the Kalman filter [5].

4.1 Kalman filter

The Kalman filter is a Bayesian estimation technique used to track stochastic dynamic systems. The filter is based on two probabilistic models :

- The system model which describes the evolution over time of the current state vector u_k . The transition between states is characterized by the known transition matrix Φ_k and the addition of Gaussian noise with a covariance Q_k .
- The measurement model which relates the measurement vector d_k to the current state through a measurement matrix H_k and the addition of Gaussian noise with a covariance R_k .

$$\begin{aligned} u_k &= \Phi_k u_{k-1} + \eta_k, \quad \eta_k \sim N(0, Q_k) \\ d_k &= H_k u_k + \xi_k, \quad \xi_k \sim N(0, R_k) \end{aligned} \quad (3)$$

Kalman filter algorithm operates in two phases : prediction and update. The prediction step consists in a state estimate extrapolation and a state covariance extrapolation :

$$\begin{aligned} \hat{u}_{k/k-1} &= \Phi_{k-1} \hat{u}_{k-1/k-1} \\ \hat{P}_{k/k-1} &= \Phi_{k-1} \hat{P}_{k-1/k-1} \Phi_{k-1}^T + Q_{k-1} \end{aligned} \quad (4)$$

Then, the predicted covariance is used to compute a new Kalman gain matrix K_k . Finally, both current covariance matrix and current state are updated :

$$\begin{aligned} K_k &= \hat{P}_{k/k-1} H_k^T [H_k \hat{P}_{k/k-1} H_k^T + R_k]^{-1} \\ \hat{u}_{k/k} &= \hat{u}_{k/k-1} + K_k [d_k - H_k \hat{u}_{k/k-1}] \\ \hat{P}_{k/k} &= (I - K_k H_k) \hat{P}_{k/k-1} \end{aligned} \quad (5)$$

The recursive process is initialized by \hat{u}_0 , an initial estimate of u , and P_0 , its error covariance matrix.

4.2 Spatio-temporal line scratch detection

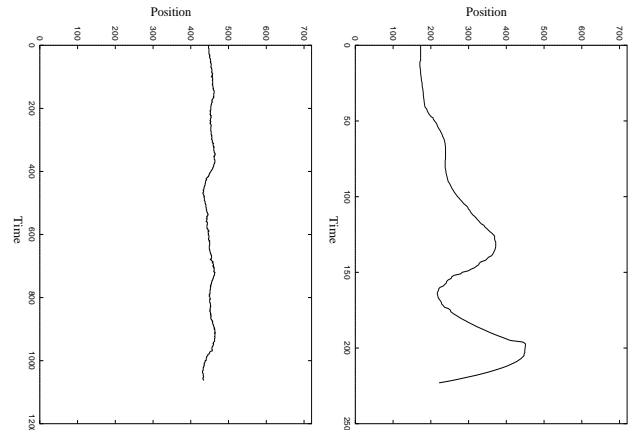


Figure 3: Line scratch tracking over 30 frames (left). Wrong detection behavior (right). Units along the x-axis are pixels, along the time axis projected stripes.

The first thing to specify when designing the Kalman filter is the representation used for the state vector.

In our case, the state vector is related to the position $x(t)$ of the vertical artifact lines over time.

Line scratches are usually generated by rubbings against rotating mechanical pieces. Therefore, they would have a sinusoidal evolution over the image sequence. Classical representation of a sinusoid is : $x(t) = A \sin(\omega t + \varphi)$. To involve Kalman filtering, we use a linear approximation of this model :

$$x(t) = A[b(t+c) - \frac{1}{3!}b^3(t+c)^3] \quad (6)$$

which integrates the well-known linear approximation of a sine curve expressed at the third order :

$$\sin(x) \simeq x - x^3/3!, \quad x \rightarrow 0 \quad (7)$$

Therefore, the state vector of our artifact line tracking system is : $u_k = (a_0 \ a_1 \ a_2 \ a_3)^t$ where a_0, a_1, a_2, a_3 denote the coefficients of our cubic polynomial model. The expression of the next state $x(t+dt)$ leads to the following transition matrix :

$$\Phi_k = \begin{pmatrix} 1 & dt & dt^2 & dt^3 \\ 0 & 1 & 2.dt & 3.dt^2 \\ 0 & 0 & 1 & 3.dt \\ 0 & 0 & 0 & 1 \end{pmatrix} \quad (8)$$

The system model is initialized using (7). The Kalman-based tracking process provides then the trajectories of the potential detected line artifacts. The examination of the obtained trajectories easily permits to distinguish between effective line artifacts (see the left profile on fig. 3) and false detections (right profile on fig. 3). Let us point out that the latter case may not occur in practice because the tracking of the corresponding line would be interrupted after a few iterations regarding to its incompatible behavior with respect to a line artifact trajectory.

5 Line scratch removal

This stage consists in post-processing the detection field. To reconstruct the corrupted pixels of the detected line scratches we use an interpolation method.

Classical image interpolation procedures falls into three main categories : intensity-based, contour-based and shape-based interpolations. In our case, we involve an intensity-based interpolation. This technique takes the original pixel intensity value and generates a new interpolated pixel intensity. The calculation of the interpolated value takes a limited number of data points within a small neighborhood. Two kinds of neighborhood may then be used :

- a spatial neighborhood extracted from the current frame,
- a spatio-temporal neighborhood extracted from the current image and the preceding and/or the following frames of the sequence.

As computing power is an important factor for old film restoration, we use a spatial neighborhood around the line scratches. Let us notice that line scratches width is limited to a few pixels, so, using only the pixels surrounding these deteriorations in the current frame seems to be sufficient for efficient interpolation.

5.1 Image interpolation methods

The first step in the design of an image interpolation algorithm is to propose a mathematical model for the luminance variation to catch a local interaction of some neighbor pixels. One can then develop a method which fits this form to the observed image.

The main interpolation models used in signal and image processing are :

- polynomial models [7], [13];
- stochastic models [14], [9], [8], [6] and
- Fourier series [3], [1].

Polynomial interpolation usually relies on splines or B-splines representations which are the basis for curve fitting [7]. The only requirement of such methods is the order of the polynomial which best fits the input signal. This is a good solution for the reconstruction of homogeneous regions. However, it fails to reconstruct regions of high activity such as textured areas because it approximates only the low frequencies of the input signal.

Stochastic models such as AutoRegressive (AR) models [6] or Markov Random Field (MRF) models [8], [9] are also widely used for spatial interpolation process. They allow a better interpolation than polynomial models. Indeed, the high frequencies which are lost in polynomial interpolation may be recovered using such stochastic interpolation procedure. However, they are difficult to implement.

Fourier series allow a simple representation of input signals either with low or/and high frequency components [3], [1]. While polynomial and stochastic models require the knowledge of the model order, the use of Fourier series only depends on the number of samples of the discrete signal.

5.2 A two-stages restoration method

To completely remove line artifacts, we propose a two-stages restoration approach which first reconstructs low frequency components and then deals with higher frequencies.

Let us emphasize that errors in the reconstruction of line scratches are more visible than in the case of blotches. Indeed, line scratches usually persist across several frames. Therefore, reconstructed line areas have to be as close as possible to the original patch.

5.2.1 Low-pass image reconstruction

Classical methods such as low-pass filters [4] or median filters [10] are not appropriate tools for old film restoration because they deteriorate high frequency components of the images. Our low-pass image reconstruction method is a polynomial interpolation based on a cubic polynomial :

$$I_{LP}(x, y) = \sum_{k=0}^3 \sum_{l=0}^3 a_{kl} x^k y^l \quad (9)$$

which is the most simple model to approximate low frequency components of an image.

To estimate the model coefficients a_{kl} , we use a least-square technique whose input data are the coordinates (x_i, y_i) of uncorrupted pixels P_i belonging to a 10×5 pixel block size \mathcal{P} around the line patch.

The resulting estimates \hat{a}_{kl} are then used to reconstruct low frequency components of the line scratch area using :

$$R_{LP}(x_j, y_j) = \sum_{k=0}^3 \sum_{l=0}^3 \hat{a}_{kl} x_j^k y_j^l, \quad (x_j, y_j) \in \mathcal{Q} \quad (10)$$

where \mathcal{Q} denotes the set of deteriorated pixels to reconstruct. Figure 4 shows, on the left, the original frame of a damaged film sequence and, on the middle, the result of our low-pass reconstruction technique on the detected line scratch. We can easily notice the perceived visibility of the interpolated line area. This phenomenon would be emphasized in a film sequence. This shows that a suitable old film restoration process must integrate a method of dealing with high frequency components which, as expected, have been lost in the present case.

5.2.2 High-pass image reconstruction

Numerous image restoration techniques exist but most of them do not or just partially deal with the high frequencies of the images. Very few research work, to our knowledge, has been devoted to this issue [14]. Furthermore, they are mainly based on the video format.

We propose a high-pass image reconstruction technique based on Fourier series. First, we extract the high frequencies from the area (pixel bloc \mathcal{P}) which has been used for the reconstruction of the low frequencies of the line artifact region. This is achieved with a simple difference :

$$I_{HP}(x_i, y_i) = I(x_i, y_i) - I_{LP}(x_i, y_i), \quad (x_i, y_i) \in \mathcal{P} \quad (11)$$

Fourier series are most likely to fit high frequencies of image profiles thanks to their oscillatory nature. Therefore, our interpolation method rely on the following model :

$$I_{HP}(x, y) = \sum_{k=0}^{N_{wx}} \sum_{l=0}^{N_{wy}} [a_{kx} \sin(\omega_{kx} x) + b_{kx} \cos(\omega_{kx} x)] \times [a_{ky} \sin(\omega_{ky} y) + b_{ky} \cos(\omega_{ky} y)] \quad (12)$$

where ω_{kx}, ω_{ky} represent the different frequencies of the model.

To illustrate our estimation method of the model coefficients $a_{kx}, b_{kx}, \omega_{kx}, a_{ky}, b_{ky}, \omega_{ky}$ let us consider the case of mono-dimensional signals. The method may then easily be extended to bi-dimensional ones.

An input signal $S(x)$ may be represented using Fourier series as :

$$S(x) = \sum_{k=0}^{N_w} a_k \sin(\omega_k x) + b_k \cos(\omega_k x) \quad (13)$$

Assuming $S(x)$ sampled at a constant period in an interval $[0, x_n]$, the model frequencies ω_k can be expressed as : $\omega_k = 2\pi k / x_n, k \in [0, x_n - 1]$.

To estimate the model coefficients a_k, b_k, ω_k , we use an iterative scheme based on the minimization of the following criterion :

$$E(a_k, b_k, \omega_k) = \sum_{x_i \in \mathcal{P}} [a_k \sin(\omega_k x_i) + b_k \cos(\omega_k x_i) - S_k(x_i)]^2 \quad (14)$$

The first step of our incremental algorithm consists in estimating the coefficients a_0, b_0, ω_0 using the model :

$$S_0(x_i) = a_0 \sin(\omega_0 x_i) + b_0 \cos(\omega_0 x_i), \quad x_i \in \mathcal{P} \quad (15)$$

Assuming $S_0(x_i) = S(x_i), x_i \in \mathcal{P}$, a Fourier transform of the signal $S_0(x)$ allows an estimation of the frequency ω_0 . Then, a least-squares technique, deriving from (15), is used to compute the two other model coefficients.

The second stage of our method relies on the decomposition of the signal $S_0(x)$ as :

$$S_1(x_i) = S_0(x_i) - [\hat{a}_0 \sin(\hat{\omega}_0 x_i) + \hat{b}_0 \cos(\hat{\omega}_0 x_i)], \quad x_i \in \mathcal{P} \quad (16)$$

This process is repeated until the value of criterion $E(\hat{a}_k, \hat{b}_k, \hat{\omega}_k)$ falls under a threshold.

A similar procedure is used to estimate the image model coefficients $\hat{a}_{kx}, \hat{b}_{kx}, \hat{\omega}_{kx}, \hat{a}_{ky}, \hat{b}_{ky}, \hat{\omega}_{ky}$. Therefore,

the high frequencies components of the line artifact area may be reconstructed. The resulting reconstructed signal $R_{HP}(x_j, y_j)$, $(x_j, y_j) \in \mathcal{Q}$, is then added to the previously computed low frequency signal $R_{LP}(x, y)$ to complete our two-stages reconstruction process. Figure 4 shows, on the right, the results of such restoration method which produces significant improvement in quality.

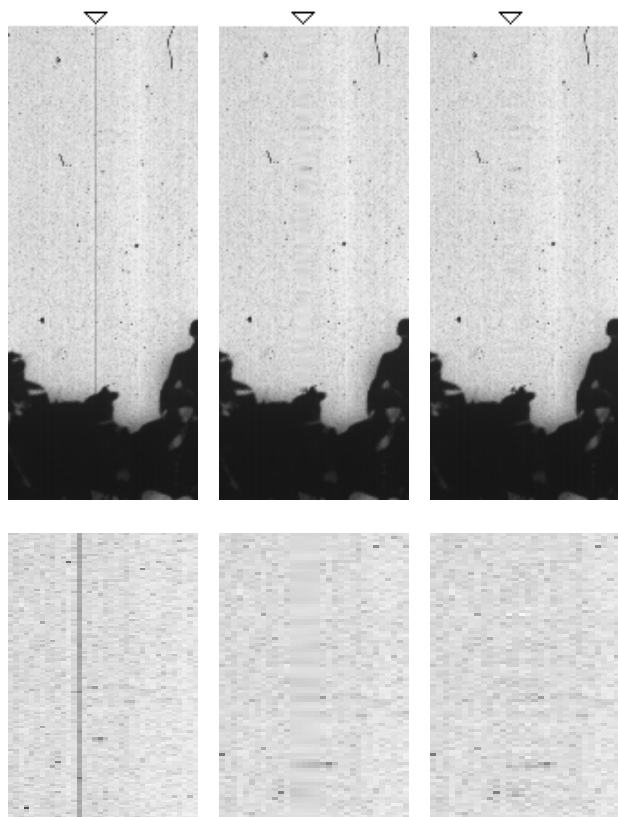


Figure 4: Frame of a film sequence (left), corresponding low frequency reconstruction (middle) and low and high frequency reconstruction (right).

6 Summary and conclusion

We have presented an efficient detector of line scratches which are common artifacts in motion picture films. This detector is based on morphological transformations and a Kalman filter is involved to track the potential scratches over the frames. Thus, false line scratches are rejected and only the damaged areas are post-processed by our reconstruction method. Our line scratches removal algorithm is a two-stages interpolation technique. The low frequencies of the deteriorated areas are first reconstructed using a simple polynomial interpolation. Then, we deal with the higher frequencies using an appropriate model for such interpolation : Fourier series. This interpolation turned out to be a powerful method leading to a nearly invisible restoration.

References

- [1] Bailey D.H., Swarztrauber P.H. The fractional Fourier transform and applications. *SIAM revue*, 33(3):389–404, September 1991.
- [2] Buisson O., Besserer B., Boukir S., Helt F. Deterioration detection for digital film restoration. *CVPR'97, Int. Conf. on Computer Vision and Pattern Recognition, Puerto Rico, USA*, 1:78–84, June 1997.
- [3] Edwards R.E. *Fourier series*. Springer-Verlag, 2nd edition, 1982.
- [4] Geman S., McClure D.E. A nonlinear filter for the film restoration and other problems in image processing. *Graphical Models and Image Processing*, 4, 1992.
- [5] Giau-Checa B., Deriche R., Viéville T., Faugeras O. Tracking segments in a monocular sequence of images. Technical report, INRIA, December 1993.
- [6] Kokaram A.C. Detection and removal of line scratches in degraded motion picture sequences. *Signal Processing VIII: theories and Application, proceedings of EUSIPCO-96, Trieste, Italy*, 1996.
- [7] Lee C.H. Restoring spline interpolation of CT images. *IEEE Trans. on Medical Imaging*, (3):142–149, September 1983.
- [8] Li S.Z., Chan K.L., Wang H. Bayesian image restoration and segmentation by constrained optimization. *CVPR'96, Int. Conf. on Computer Vision and Pattern Recognition*, pages 1–6, 1996.
- [9] Morris R.D. *Image sequence restoration using Gibbs distributions*. PhD thesis, University of Cambridge, May 1995.
- [10] Pitas I., Venetsanopoulos A.N. *Nonlinear digital filters principles and applications*. Kulwer academic publishers, 1990.
- [11] Sanz J.L.C., Hinkle E.B., Jain A.K. *Radon and projection, transform-based, computer vision*. Springer-Verlag, June 1987.
- [12] Serra J. *Image analysis and mathematical morphology*. Academic press, 1982.
- [13] Unser M. et al. Fast B-spline transforms for continuous image representation and interpolation. *IEEE Trans. on Pattern Analysis and Machine Intelligence*, 13(3):277–285, March 1991.
- [14] Veldhuis R. *Restoration of lost samples in digital signals*. Prentice Hall, 1990.